

# Cascade Pattern Recognition Structure for Improving Quantitative Assessment of Estrogen Receptor Status in Breast Tissue Carcinomas

Spiros Kostopoulos, M.Sc., Dionisis Cavouras, Ph.D., Antonis Daskalakis, M.Sc., George C. Kagadis, Ph.D., Ioannis Kalatzis, Ph.D., Pantelis Georgiadis, M.Sc., Panagiota Ravazoula, M.D., and George Nikiforidis, Ph.D.

**OBJECTIVE:** To develop and validate a computer-based approach for the quantitative assessment of estrogen receptor (ER) status in breast tissue specimens for breast cancer management.

**STUDY DESIGN:** Microscopy images of 32 immunohistochemically (IHC) stained specimens of breast cancer biopsies were digitized and were primarily assessed for ER status (percentage of positively stained nuclei) by a histopathologist. A pattern recognition system was designed for automatically assessing the ER status of the IHC-stained specimens. Nuclei were automatically segmented from background by a pixel-based unsupervised clustering algorithm and were characterized as positively stained or unstained by a supervised classification algorithm. This cascade structure boosted the system's classification accuracy.

**RESULTS:** System performance in correctly characterizing the nuclei was 95.48%. When specifying each case's ER status, system performance was statistically not significantly different to the physician's assessment ( $p = 0.13$ ); when ranking each case to a particular 5-scale ER-scoring system (giving the chance of response to endocrine treatment), the system's score and the physician's score were in agreement in 29 of 32 cases.

**CONCLUSION:** The need for reliable and operator independent ER-status estimation procedures may be served by the design of efficient pattern recognition systems to be employed as support opinion tools in clinical practice. (Anal Quant Cytol Histol 2008;30:218–225)

**Keywords:** estrogen receptors; histopathology; image analysis; pattern recognition.

From Medical Image Processing and Analysis Group, Laboratory of Medical Physics, School of Medicine, University of Patras; Department of Pathology, University Hospital, Rio; and Department of Medical Instrumentation Technology, Technological Education Institution of Athens, Athens, Greece.

Messrs. Kostopoulos, Daskalakis and Georgiadis are Ph.D. Candidates, Medical Image Processing and Analysis Group, Laboratory of Medical Physics, School of Medicine, University of Patras.

Dr. Cavouras is Professor, Department of Medical Instrumentation Technology, Technological Education Institution of Athens.

Dr. Kagadis is Postdoctoral Researcher, Medical Image Processing and Analysis Group, Laboratory of Medical Physics, School of Medicine, University of Patras.

Dr. Kalatzis is Postdoctoral Researcher, Department of Medical Instrumentation Technology, Technological Education Institution of Athens.

Dr. Ravazoula is Medical Doctor, Department of Pathology, University Hospital.

Dr. Nikiforidis is Professor, Medical Image Processing and Analysis Group, Laboratory of Medical Physics, School of Medicine, University of Patras.

Address correspondence to: Spiros Kostopoulos, M.Sc., Medical Image Processing and Analysis Group, Laboratory of Medical Physics, School of Medicine, University of Patras, 26500 Rio, Greece (skostopoulos@upatras.gr).

**Financial Disclosure:** Mr. Kostopoulos was supported by a grant from the Greek State Scholarships Foundation (IKY).

According to the World Health Organization, the most frequent neoplasm in females is breast cancer.<sup>1</sup> Breast cancer cells can express a variety of hormone receptors. Estrogens are hormones that affect breast tissues (normal or malignant) by binding to estrogen receptors (ERs) and by causing cells to grow or divide. Even though the latter is a normal route of breast development, it can potentially lead to the development of cancer cells.<sup>2</sup> Therapeutic management and treatment of women with breast cancer cells expressing ERs (positive ER-status) differs from those with negative ER status.<sup>2</sup> Consequently, ER status has been proposed as a biologic factor to predict the clinical response of hormonal therapy.<sup>3</sup>

Traditionally ER status has been assessed by biochemical methods. Recently the method of choice is immunohistochemistry (IHC).<sup>4</sup> According to recommendations by the American Society of Clinical Oncology, ER status should be reported as the percentage of positive nuclei.<sup>5</sup> The histopathologist microscopically assesses ER status by inspecting the concentration of positively stained nuclei within areas of high positively stained nuclei. Those areas are characterized as high-power fields or fields most representative for ER-staining.<sup>6</sup> It is apparent that, because such assessment might be affected by the physician's experience, an objective quantification of the ER status might be of value in reducing interobserver and intraobserver variability.<sup>5</sup>

Previous studies<sup>5-10</sup> have employed computer-aided image analysis methods for quantifying the ER-status of breast cancer. Diaz et al<sup>5</sup> used a commercially available image analysis system (QCA, Lake Bluff, Illinois, U.S.A.) for determining the percentage of positive IHC-stained tumor cells by using colorimetric algorithms. Bejar et al<sup>9</sup> used a different image analysis system (Wscannary, Galai Corp, Migdal-HaEmek, Israel) for measuring the nuclei's optical density and computing a weighted score for separation of ER-positive from ER-negative breast carcinomas. Both Diaz et al<sup>5</sup> and Bejar et al<sup>9</sup> achieved good agreement with observers' score ( $\kappa = 0.84$  and  $0.89$ , respectively). Mofidi et al<sup>6</sup> and Lehr et al<sup>10</sup> employed functions of Photoshop image-processing software (Adobe Systems, Mountain View, California, U.S.A.) to assess ER status—Mofidi et al<sup>6</sup> by evaluating the H-score index, a combination of positively stained nuclei percentage and of nuclei staining intensity, and Lehr et al<sup>10</sup> by evaluating the immunocytochemical index. Their findings showed acceptable ( $r=0.84$ ) to marginal

( $r=0.76$ ) correlations against the pathologists' evaluation. Kohlberger et al<sup>8</sup> used color thresholds to determine the proportion of stained nuclear area, and they have reported marginal correlation (Spearman's  $r=0.64$ ) with physicians H-score. Schnorrenberg et al<sup>7</sup> proposed a different approach, based on pattern recognition for simulating the way that pathologists evaluate individual cells. They implemented a modular neural network algorithm using 2 features—average intensity and texture measure—for classifying nuclei, and they have assessed the ER status by the H-score index, achieving the highest overall accuracy (84%) against the physicians' evaluation. It is obvious that any effort to improve the precision of computer-aided ER status quantification would require more rigorous image analysis methods.

The contribution of the present study lies in the employment of state-of-the-art pattern recognition methods and color textural features to design a complex nuclei classification system for ER status quantification. In particular, the complexity of the design lies in interfacing an efficient unsupervised clustering algorithm, the fuzzy c-means (FCM),<sup>11</sup> with a fast and optimally designed classifier, the Probabilistic Neural Network (PNN),<sup>12</sup> to locate and discriminate with accuracy either positively or negatively stained nuclei from background tissue, thus leading to automatic assessment of the ER status through the concentration of positive nuclei present in the IHC-stained specimen.

## Material and Methods

### Material

Thirty-two formalin-fixed, paraffin-embedded, IHC-stained biopsy specimens of breast cancer were collected by an experienced histopathologist (P.R.) from the archives of the Department of Pathology of the University Hospital of Patras, Rio, Greece. For each specimen, the ER expression was semiquantitatively assessed following a simplified version of a clinical scoring protocol<sup>13</sup> (Table I). Accordingly,

**Table I** Scoring System Employed in the Present Study

Score	Proportion of nuclear staining (%)
0	0–5
1	6–10
2	11–33
3	34–66
4	67–100

following the daily clinical routine, the concentration of positively stained nuclei—brown colored—to the total number of positively and negatively stained nuclei—blue colored—was estimated by visual inspection of microscopic fields, in which a large number of positively stained nuclei existed. Percentage scores were then referred to the clinical scoring protocol for labeling each case's chance of response to endocrine treatment, as shown in Table I. The cut-off value for positive status was set at 5%.

#### Image Acquisition

From the same specimen regions on which the histopathologist's clinical assessment was based, 5 non-overlapping images ( $1300 \times 1030 \times 36$  bit) were selected on average from each case and were digitized at a magnification of  $\times 400$  using a Zeiss Axiostar-Plus light microscope (Zeiss, Göttingen, Germany) and a Leica DC 300F color video camera (Leica, Wetzlar, Germany). Images were acquired using the Leica IM50 image manager software that accompanied the Leica microscope. Parameters regarding exposure time, image amplification, image contrast,  $\gamma$  value and white balance were automatically adjusted by the provided software. To alleviate light fluctuations, the microscope was turned on a few minutes before image capturing, in order to reach thermal equilibrium.

#### System Design

The system implemented the FCM clustering algorithm in conjunction with the PNN algorithm to form a cascade unsupervised-supervised classification structure as illustrated in Figure 1. The cascade structure comprised 3 basic stages: nuclei segmentation, feature extraction, and nuclei classification. The result was automatic identification of positively and negatively stained nuclei, quantification of the specimen's ER-status from the concentration of positively stained nuclei, and reference to a scoring scale employed by physicians in clinical practice.

**Nuclei Segmentation by FCM.** The original RGB image (Figure 2) was temporarily converted into the  $L^*a^*b^*$  color space (see Appendix).  $L^*$  represents the difference between light and dark intensities;  $a^*$  represent the difference between redness and greenness; and  $b^*$  represents the difference between blueness and yellowness.<sup>14</sup> By this approach, chromaticity was separated from intensity.<sup>15</sup> Consequently images were transformed from RGB into 2-color images, channels  $a^*$  and  $b^*$ , rendering information processing easier.

The FCM unsupervised clustering algorithm, which requires no training, was implemented for partitioning the image-pixels into 3 clusters or classes—pixels accounting for brown nuclei, pixels

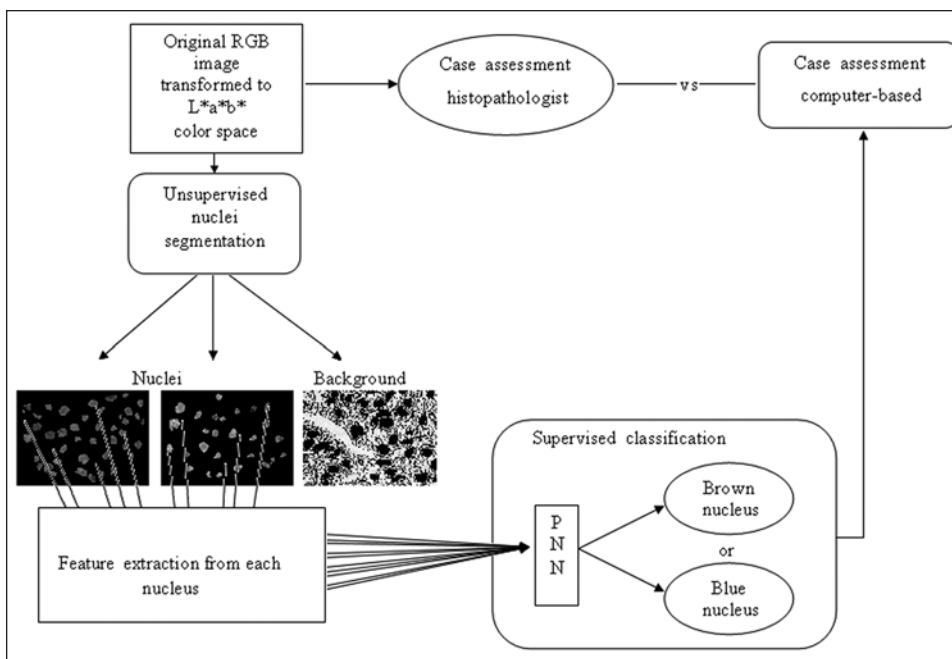


**Figure 1** Schematic representation of system design.  $L^*$  = difference between light and dark intensities,  $a^*$  = difference between redness and greenness,  $b^*$  = difference between blueness and yellowness, RGB = red-green-blue.

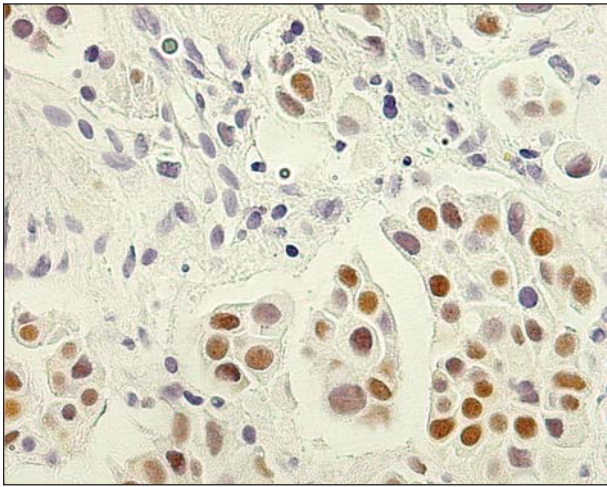


Figure 2 Original RGB image.

accounting for blue nuclei and pixels accounting for the remaining tissue background. The FCM follows an iterative procedure in which image-pixels, represented by 2 features (intensity of  $a^*$  and  $b^*$  channel), get fuzzy allocation to a cluster according to distance metric criteria. Features were normalized to zero mean value and unit variance<sup>17</sup> according to relation (equation 2).

The algorithm iteratively facilitates for minimization of the objective function (equation 1)

$$J(M,C) = \sum_{i=1}^N \sum_{j=1}^C m_{ij}^w \|x_i - c_j\|^2 \quad (1)$$

to provide solution for the membership function matrix  $M$  and cluster center matrix  $C$ , where  $m_{ij} \in \{0,1\}$  is the degree of membership of  $x_i$  image-pixel in the cluster  $j$ ,  $\|x_i - c_j\|$  is the Euclidean distance between  $j$ -th cluster center and  $i$ -th image-pixel, and  $w \in [1,\infty]$  is the fuzzy exponent, which determines the degree of fuzziness. The algorithm converges when  $|m_{ij}^{k+1} - m_{ij}^k| < \epsilon$ , where  $\epsilon \in (0,1)$  is a termination criterion and  $k$  is the iteration steps.

Because the most populated cluster corresponded to tissue-background in all cases, it could be easily isolated and discarded. Image-pixels residing in the other 2 clusters were used to form 2 new images with potentially either brown or blue pixels (Figure 3). Both brown and blue images were further processed for eliminating noisy regions by morphologic operators, which comprised image closing (erosion followed by dilation), fill holes, and image opening (dilation followed by erosion),<sup>16</sup> and by a size filter for retaining only objects (nuclei) larger than 300

pixels. Finally, images were combined (logical *and* operation) with the original RGB image for obtaining the final segmented image, in which each segmented nucleus had RGB texture (Figure 3). These images and the original were presented to the expert histopathologist for evaluating the correctness of nuclei identification at this preliminary stage of nuclei labeling. The result of such an assessment led us to employ more drastic measures, such as unsupervised-supervised classification in a cascade mode (FCM/PNN).

*Feature Extraction.* Five features—mean value, SD, skewness, kurtosis and color range—were calculated from each R, G and B nucleus intensity histogram, thus forming a total of 15 features of texture for each nucleus. Features were normalized to zero mean value and unit variance,<sup>17</sup> considering all brown and blue nuclei, according to relation (equation 2)

$$\tilde{x}_i = \frac{x_i - \mu}{s} \quad (2)$$

where  $x_i$  and  $\tilde{x}_i$  are the feature vectors prior to and after the normalization,  $\mu$  is the mean value of each feature and  $s$  is the SD of each feature.

*Nuclei Classification by PNN.* Segmented nuclei, represented by a 15-dimensional feature vector, were fed into an optimally designed PNN classifier, which was used for discriminating between brown and blue nuclei. The PNN discriminant function is given (equation 3):

$$g_j(x) = \frac{1}{(2\pi)^{d/2} \sigma^d N_j} \sum_{i=1}^{N_j} \frac{1}{1 + \|x - x_i\|^2 / \sigma^2} \quad (3)$$

where  $\sigma$  is the smoothing parameter (experimentally determined to be 0.27),  $N$  is the number of nuclei (patterns or feature vectors) forming class  $j$ ,  $d$  is the feature vector dimensionality,  $x_i$  is the  $i$ -th feature vector of class  $j$ , and  $x$  is the unknown feature vector. The PNN classifies the input vector to the class with the highest decision function.

The PNN classifier was designed using an adequate number of nuclei, randomly chosen from the first 22 cases in Table II, which the expert physician had previously classified as brown (714) or blue (1,117). These nuclei constituted the gold standard dataset that was employed in the optimum design and evaluation of the PNN by means of the  $k$ -fold cross-validation process. Data were randomly split into 10 ( $k = 10$ ) non-overlapping subsets of approx-

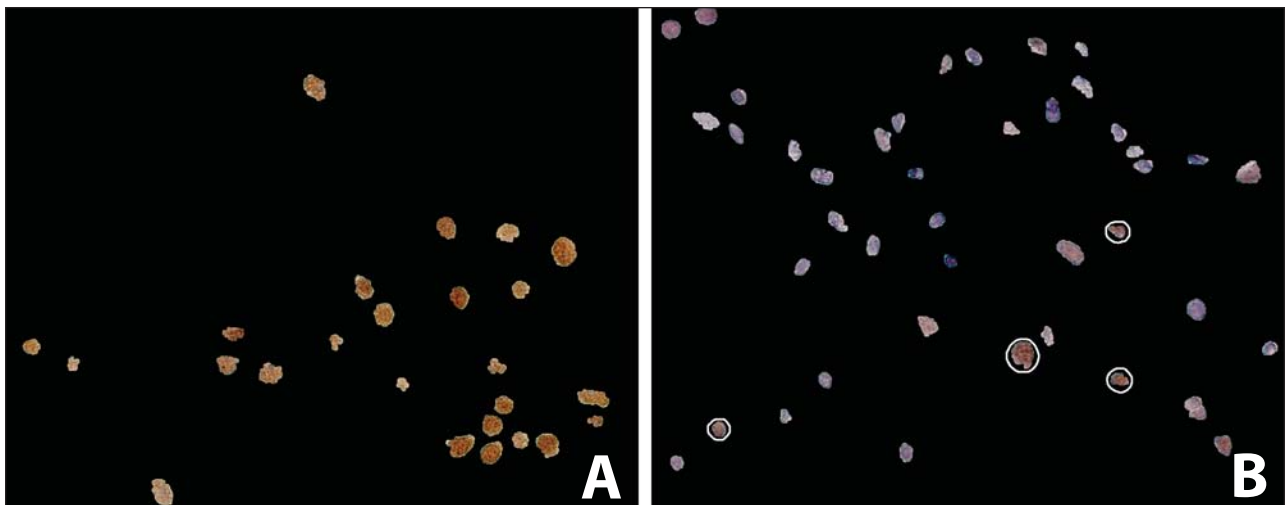


**Figure 3** Segmented (A) brown and (B) blue nuclei. White encircled nuclei, while initially incorrectly estimated as blue by the FCM, were correctly classified as brown by the PNN.

imately equal size. The PNN was trained on the  $k-1$  of these subsets (training set), combining the subsets' features using the "exhaustive search" methodology and was tested with the 1 remaining subset (testing set) to obtain an estimate of the classification error.<sup>18</sup> Exhaustive search was carried out to determine the best feature-vector combination that led to the maximum classification accuracy.<sup>19</sup> The best feature combination was regarded that which gave maximum classification accuracy with the least number of features.

**System Operation.** The designed system operated on a new case's digitized images extracted from high-power fields of the case's specimen according to the following steps:

1. Images were automatically segmented.
2. Nuclei were identified, and the optimal set of features was calculated from each nucleus.
3. Nuclei were labelled by the PNN as brown or blue.
4. The case's ER status was calculated and a score was determined, indicating the response to endocrine treatment.

#### System Evaluation

The results of the proposed system were evaluated against the physician's findings in terms of nuclei classification, ER status and case score for response to endocrine treatment.

System nuclei classification accuracy was assessed by the physician, who examined a large number of nuclei that were labeled brown and blue by the system and evaluated the system's precision by relation (equation 4):

$$\% \text{ Accuracy} = \frac{TP}{TP + FN} \times 100 \quad (4)$$

where  $TP$  are nuclei correctly categorized by the system and  $FN$  are misclassified nuclei.

The system's ER status proximity to the physician's assessment was tested by means of the Kolmogorov-Smirnov<sup>20</sup> nonparametric test. The agreement of the system's case score to the physician's score, using the scoring system of Table I, was examined by means of the Kendall's coefficient of concordance<sup>21</sup> (KCC).

#### Results

In the preliminary stage of nuclei segmentation by the FCM (see *Nuclei Segmentation by FCM* section), 2,057 objects were segmented, of which 89.3% were identified by the physician as nuclei (714 brown and 1,117 blue). These nuclei constituted the gold standard for the design of the PNN classifier. The classifier was optimally designed by the exhaustive search and the  $k$ -fold cross-validation methods (see *Nuclei Classification by PNN* section). Feature combinations that gave the mean maximum accuracy (average of 100 repetitions of 10-fold cross-validation)

**Table II** Comparative Evaluation of the ER Status and Score Between the Expert Physician and the Proposed System

Case	Physician's evaluation (%)	System evaluation (%)	Physician's ER score	System's ER score
1	40	37.02	3	3
2	70	63.41	4	3
3	80	77.28	4	4
4	90	77.38	4	4
5	70	72.63	4	4
6	70	74.21	4	4
7	90	93.62	4	4
8	70	67.27	4	4
9	30	15.61	2	2
10	40	36.19	3	3
11	30	29.35	2	2
12	40	42.66	3	3
13	60	37.00	3	3
14	20	19.41	2	2
15	40	28.11	3	2
16	70	78.08	4	4
17	80	74.02	4	4
18	90	88.87	4	4
19	90	87.54	4	4
20	30	17.49	2	2
21	70	73.05	4	4
22	90	88.00	4	4
23	80	77.82	4	4
24	30	16.48	2	2
25	50	64.80	3	3
26	60	33.56	3	3
27	80	67.42	4	4
28	80	52.31	4	3
29	90	67.67	4	4
30	90	85.77	4	4
31	90	72.76	4	4
32	85	79.53	4	4

ER = estrogen receptor.

for each exhaustive search step (i.e., combination per 2, 3, 4, 5 and 6) are shown in Figure 4. The mean maximum accuracy gradually increased from 94.22% (2 features) to 95.48% (6 features). Due to insignificant variations in accuracies, the best 4-feature combination was chosen for the design of the PNN and comprised the mean value of red channel, mean value of blue channel, range of green channel and range of blue channel.

Regarding the evaluation of the system for nuclei classification, the physician examined the system's output in characterizing 513 nuclei taken from 3 arbitrarily selected images that had not been employed in the design of the PNN (last 10 cases in Table II). Table III shows the system's overall accu-

racy (91.4%) in correctly discriminating brown nuclei from blue nuclei. Moreover, in order to assess the accuracy of the proposed system in estimating the proportion of nuclei in individual cases, a comparative evaluation with the physician was performed. Accordingly, the physician determined manually the number of brown nuclei and blue nuclei that were contained in the digitized images of the 10 cases not involved in the design of the system. The system's accuracy ranged between 88.4% and 96.8%, with mean  $92.9 \pm 2.8\%$ , based on an average of 310 nuclei per case.

Concerning system performance for ER-status assessment, the Kolmogorov-Smirnov test revealed that there were no statistically significant divergences from the physician's evaluations ( $p=0.13$ ). Table II presents the ER status scores.

Finally, the level of agreement between the system and the physician in assigning scores to cases that indicated the response to endocrine treatment can be estimated from Table II. Overall, agreement existed in 90.63% of the cases and in particular in 100% (5/5), 85.7% (6/7) and 90% (18/20) for levels 2, 3 and 4, respectively, of the scoring protocol. The KCC test showed a strong agreement ( $W=0.898$ ,  $p<0.001$ ).

**Discussion**

ER status is reported as an important variable for

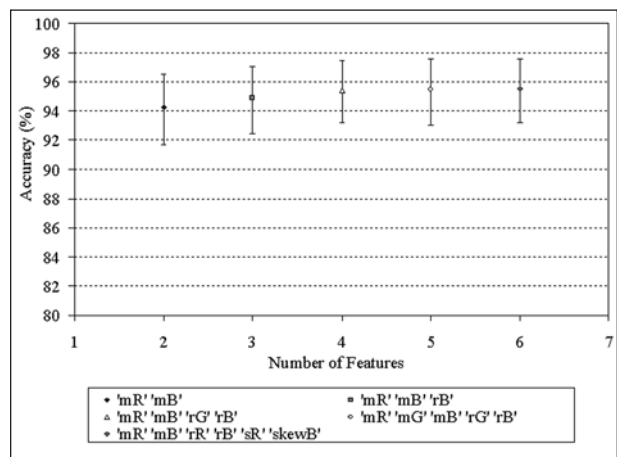


**Figure 4** Variation of highest PNN precision in classifying nuclei against the number of features employed. The span of accuracies refers to the ranges of accuracies achieved by the 10-fold cross-validation method. Also shown (inset) are best feature combinations. m = mean, r = range, s = SD, skew = skewness, R = red channel, G = green channel, B = blue channel.

**Table III** Comparative Evaluation (Physician vs. System) in Characterizing Nuclei as Brown or Blue, Employing 3 Arbitrary Selected Images from Different Cases not Involved in the Design of the System

System	Physician		Accuracy (%)
	Brown	Blue	
Brown	183	23	88.83
Blue	21	286	93.16
Overall accuracy			91.42

prognostic and predictive evaluation of breast cancer.<sup>2,3</sup> In everyday clinical routine, ER status is estimated as the percentage of positively stained nuclei to the total number of nuclei in the specimen, usually performed by visual inspection of regions with high concentration of positive nuclei. The necessity for standardization of the post-analytical scoring and quantification of ER status by means of IHC staining is still an open field of research.<sup>22</sup> A diversity of image analysis methods, such as commercially available packages and custom made algorithms, have been studied for the quantification of IHC-stained sections.<sup>5-7,9,10</sup> In the present study, a high performance computer-based system is proposed for the objective identification of the ER status of breast carcinomas, incorporating state-of-the-art pattern recognition methods (a clustering algorithm in cascade with a PNN classifier) and color textural features.

Nuclei were initially segmented by employing the FCM unsupervised algorithm using as features the chromaticity,  $a^*$  and  $b^*$ , of the  $L^*a^*b^*$  color space.<sup>23</sup> Evaluation of the segmentation stage revealed that the system identified correctly 89.3% of the nuclei, which is in line with the findings of previous studies.<sup>24-27</sup> For increasing the precision, a PNN classifier was employed, in cascade with the FCM. The PNN was optimally designed from information obtained from the FCM (textural features from segmented nuclei). The PNN looked at the result of the FCM and refined the nuclei segmentation process by reassigning them to either brown or blue classes. This measure increased nuclei classification accuracy to about 95% (Figure 4) and the agreement with the physician on characterizing nuclei as brown or blue to 91.4% (Table III). In addition, the system's accuracy in determining the proportion of brown or blue nuclei in individual cases was 92.9%, with an SD of 2.8%. The result of the nuclei segmentation procedure is shown in Figure 3. As it may be noted, encircled nuclei that were falsely la-

beled blue by the FCM were in turn correctly characterized as brown by the PNN.

The proposed system's quantification of ER status was compared against the histopathologist's reported semiquantitative assessment, revealing a high degree of correlation (Spearman's  $r = 0.87$ ). Corresponding findings in earlier studies<sup>5-9</sup> have shown different degrees of correlation ranging from satisfactory (such as Spearman's  $r = 0.64$  in<sup>8</sup>) to high (such as pairwise  $\kappa = 0.84$  in<sup>5,6</sup>) between their image analysis methodologies and the physicians' assessments. It must be noted that it is difficult to draw concrete conclusions regarding direct comparisons between systems due to the absence of reliable and universal gold standards.

The performance of the proposed system was also evaluated by means of a 5-scale ER ranking clinical protocol, which gives the probability of each case's response to endocrine treatment. High agreement was found with the physician's score (29 of 32 cases [90.6%] and KCC = 0.898,  $p < 0.001$ ). The wrongly ranked cases may be due to the variability in the staining among cases. Previous studies have also reported results by means of various ER ranking protocols. Schnorrenberg et al<sup>7</sup> have indicated up to 84% overall accuracy in correctly ranking their cases to the H-score. Lehr et al<sup>10</sup> have presented adequate correlation ( $r = 0.76$ ) of computer-based immunostaining intensity with enzyme immunoassay findings.

In conclusion, the proposed system operates in an automatic manner, achieving high accuracies even when engaged in new cases. This may be indicative of the system's capability for application in a clinical environment. The high rate of accuracy may be attributed to interfacing in cascade a clustering algorithm with a PNN classifier for characterizing nuclei and, thus, for quantifying with precision each case's ER status. The system has the potential to serve as an operator-independent support opinion tool in clinical practice.

## Appendix

According to the Commission International de l'Éclairage, the coordinates of the  $L^*a^*b^*$  color space are derived by a nonlinear transformation of the 3 primary colors  $X$ ,  $Y$  and  $Z$ . The linear transformation of RGB space to  $X$ ,  $Y$  and  $Z$  is defined as:<sup>28</sup>

$$\begin{pmatrix} X \\ Y \\ Z \end{pmatrix} = \begin{pmatrix} 0.607 & 0.174 & 0.200 \\ 0.299 & 0.587 & 0.114 \\ 0.000 & 0.066 & 1.116 \end{pmatrix} \begin{pmatrix} R \\ G \\ B \end{pmatrix}$$

$$L^* = 116 \left( \sqrt[3]{\frac{Y}{Y_o}} \right) - 16$$

$$a^* = 500 \left[ \sqrt[3]{\frac{X}{X_o}} - \sqrt[3]{\frac{Y}{Y_o}} \right]$$

$$b^* = 200 \left[ \sqrt[3]{\frac{Y}{Y_o}} - \sqrt[3]{\frac{Z}{Z_o}} \right]$$

## References

- Stewart BW, Kleihues P (editors): World Cancer Report. Lyon, France, IARC Press, 2003
- Diaz LK, Sneige N: Estrogen receptor analysis for breast cancer: Current issues and keys to increasing testing accuracy. *Adv Anat Pathol* 2005;12:10–19
- Jasani B, Douglas-Jones A, Rhodes A, Wozniak S, Barrett-Lee PJ, Gee J, Nicholson R: Measurement of estrogen receptor status by immunocytochemistry in paraffin wax sections. *Methods Mol Med* 2006;120:127–146
- Bejar J, Sabo E, Eldar S, Lev M, Misselevich I, Boss JH: The prognostic significance of the semiquantitatively determined estrogen receptor content of breast carcinomas: A clinicopathological study. *Pathol Res Pract* 2002;198:455–460
- Diaz LK, Sahin A, Sneige N: Interobserver agreement for estrogen receptor immunohistochemical analysis in breast cancer: A comparison of manual and computer-assisted scoring methods. *Ann Diagn Pathol* 2004;8:23–27
- Mofidi R, Walsh R, Ridgway PF, Crotty T, McDermott EW, Keaveny TV, Duffy MJ, Hill AD, O'Higgins N: Objective measurement of breast cancer oestrogen receptor status through digital image analysis. *Eur J Surg Oncol* 2003;29:20–24
- Schnorrenberg F, Tsapatsoulis N, Pattichis CS, Schizas CN, Kollias S, Vassiliou M, Adamou A, Kyriacou K: Improved detection of breast cancer nuclei using modular neural networks. *IEEE Eng Med Biol Mag* 2000;19:48–63
- Kohlberger PD, Breitenacker F, Kaider A, Löscher A, Gitsch G, Breitenacker G, Kieback DG: Modified true-color computer-assisted image analysis versus subjective scoring of estrogen receptor expression in breast cancer: A comparison. *Anticancer Res* 1999;19:2189–2193
- Bejar J, Sabo E, Misselevich I, Eldar S, Boss JH: Comparative study of computer-assisted image analysis and light-microscopically determined estrogen receptor status of breast carcinomas. *Arch Pathol Lab Med* 1998;122:346–352
- Lehr HA, Mankoff DA, Corwin D, Santeusano G, Gown AM: Application of photoshop-based image analysis to quantification of hormone receptor expression in breast cancer. *J Histochem Cytochem* 1997;45:1559–1565
- Jain AK: Fundamentals of Digital Image Processing. Englewood Cliffs, New Jersey, Prentice-Hall, 1989
- Specht DF: Probabilistic neural networks. *Neural Networks* 1990;3:109–118
- Leake R, Barnes D, Pinder S, Ellis I, Anderson L, Anderson T, Adamson R, Rhodes T, Miller K, Walker R: Immunohistochemical detection of steroid receptors in breast cancer: A working protocol. UK Receptor Group, UK NEQAS, The Scottish Breast Cancer Pathology Group, and The Receptor and Biomarker Study Group of the EORTC. *J Clin Pathol* 2000;53:634–635
- CIE Technical Report, Colorimetry, Publ. CIE 15.2-1986, CIE Central Bureau, Vienna, Austria
- Paschos G, Petrou M: Histogram ratio features for color texture classification. *Pattern Recognition Letters* 2003;24:309–314
- Gonzalez R, Woods R: Digital Image Processing. Second edition. New York, Prentice-Hall, 2002, pp 519–559
- Theodoridis S, Koutroumbas K: Pattern Recognition. Second edition. San Diego, Elsevier, 2003
- Ambroise C, McLachlan GJ: Selection bias in gene extraction on the basis of microarray gene-expression data. *Proc Natl Acad Sci U S A* 2002;99:6562–6566
- Jain AK, Duin R, Mao J: Statistical pattern recognition: A review. *IEEE Trans Pattern Anal Mach Intell* 2000;22:4–37
- Soong TT: Fundamentals of Probability and Statistics for Engineers. Chichester, West Sussex, England, Wiley, 2004
- Fleiss JL: Statistical Methods for Rates and Proportions. Second edition. New York, Wiley & Sons, 1981
- Taylor CR, Levenson RM: Quantification of immunohistochemistry: Issues concerning methods, utility and semi-quantitative assessment: II. *Histopathology* 2006;49:411–424
- Kostopoulos S, Cavouras D, Daskalakis A, Ravazoula P, Nikiforidis G: Image Analysis System for Assessing the Estrogen Receptor's Positive Status in Breast Tissue Carcinomas. *In Proceedings of International Special Topic Conference on Information Technology in Biomedicine, Ioannina, Greece, October 26–28, 2006*
- Glotsos D, Spyridonos P, Petalas P, Cavouras D, Ravazoula P, Dadioti PA, Lekka I, Nikiforidis G: Computer-based malignancy grading of astrocytomas employing a support vector machine classifier, the WHO grading system and the regular hematoxylin-eosin diagnostic staining procedure. *Anal Quant Cytol Histol* 2004;26:77–83
- Latson L, Sebek B, Powell KA: Automated cell nuclear segmentation in color images of hematoxylin and eosin-stained breast biopsy. *Anal Quant Cytol Histol* 2003;25:321–331
- Spyridonos P, Cavouras D, Ravazoula P, Nikiforidis G: Neural network-based segmentation and classification system for automated grading of histologic sections of bladder carcinoma. *Anal Quant Cytol Histol* 2002;24:317–324
- Markopoulos C, Karakitsos P, Botsoli-Stergiou E, Pouliakis A, Ioakim-Lioffi A, Kyrkou K, Gogas J: Application of the learning vector quantizer to the classification of breast lesions. *Anal Quant Cytol Histol* 1997;19:453–460
- Cheng H-D, Sun Y: A hierarchical approach to color image segmentation using homogeneity. *IEEE Trans Image Process* 2000;9:2071–2082